

XMM-Newton observations of Nova Sgr 1998

M. Hernanz

*Institut de Ciències de l'Espai (CSIC-IEEC), Campus Universitat Autònoma de Barcelona,
Facultat de Ciències, Torre C5 - parell - 2a planta, E-08193 Bellaterra (Barcelona), Spain;
hernanz@ieec.uab.es*

and

G. Sala

*Max-Planck-Institut für extraterrestrische Physik, Postfach 1312, D-85741, Garching,
Germany and Institut de Ciències de l'Espai (CSIC-IEEC); gsala@mpe.mpg.de*

ABSTRACT

We report on X-ray observations of Nova Sagittarius 1998 (V4633 Sgr), performed with XMM-Newton at three different epochs, 934, 1083 and 1265 days after discovery. The nova was detected with the EPIC cameras at all three epochs, with emission spanning the whole energy range from 0.2 to 10 keV.

The X-ray spectra do not change significantly at the different epochs, and are well fitted for the first and third observations with a multi-temperature optically thin thermal plasma, while lower statistics in the second observations lead to a poorer fit. The thermal plasma emission is most probably originated in the shock heated ejecta, with chemical composition similar to that of a CO nova. However, we can not completely rule out reestablished accretion as the origin of the emission. We also obtain upper limits for the temperature and luminosity of a potential white dwarf atmospheric component, and conclude that hydrogen burning had already turned-off by the time of our observations.

Subject headings: stars: individual (V4633 Sagittarius) — stars: novae, cataclysmic variables — stars: white dwarfs — X-rays: binaries — X-rays: individual (V4633 Sagittarius)

1. Introduction

Nova Sgr 1998 (V4633 Sgr) was discovered by Liller (1998) on 1998 March 22.3 UT, with magnitude 7.8, and it was confirmed spectroscopically by Della Valle et al. (1998) two days

later, with relatively low expansion velocities and presence of iron, thus indicating that the nova belonged to the Fe II class (Williams 1992). The nova light curve (Liller & Jones 1999) indicated that it was moderately fast, with $t_2 \approx 28$ days and $t_3 \approx 55$ days. No indication of optical polarization was found in further observations by Ikeda, Kawabata & Akitaya (2000). Lipkin et al. (2001) performed optical observations during the period 1998–2000, which revealed two photometric periodicities; the shorter and constant period of 3.014 h was interpreted as the orbital period, whereas the longer and slightly variable period of 3.08 h could be interpreted as the spin period of the white dwarf, in a nearly synchronous magnetic system. Near-infrared spectroscopy, in the range 0.8 to 2.5 μm , obtained 525 and 850 days after peak brightness by Lynch et al. (2001), revealed some symmetric lines with widths (FWHM) of 1800 km/s. There was no evidence of dust formation and the shell was hydrogen-deficient. The reddening was very uncertain ($E(B-V)=0.3 \pm 0.2$, yielding $A_V = 0.9 \pm 0.6$ for $R=3.1$), thus leading to a very uncertain distance, $d \sim 9$ kpc ($d=8.9 \pm 2.5$ kpc, Lipkin et al. (2001)).

Nova Sgr 1998 was one of the targets included in our monitoring programme of recent galactic novae in X-rays, during the first cycle of the XMM-Newton satellite. The main goal of our observations was to determine the turn-off times of hydrogen burning. Novae are the consequence of explosive hydrogen burning, through a thermonuclear runaway, on top of an accreting white dwarf in a close binary system, of the cataclysmic variable type. It is theoretically predicted that novae return to hydrostatic equilibrium after the ejection of a fraction of the accreted envelope. X-ray emission in post-outburst novae can arise through three different mechanisms. First, as the envelope mass is depleted, the photospheric radius decreases at constant bolometric luminosity (close to the Eddington value) with an increasing effective temperature. This leads to a hardening of the spectrum from optical through ultraviolet, extreme ultraviolet and finally soft X-rays, with the post-outburst nova emitting as a supersoft source with a hot white dwarf atmosphere spectrum. The duration of this soft X-ray emission is related to the nuclear burning timescale of the remaining H-rich envelope (see, for instance, Table 1 in Gehrz et al. (1998)) and depends among other factors on the white dwarf mass (Tuchman & Truran 1998; Sala & Hernanz 2005a,b). The second site of X-ray emission in post-outburst novae is the ejected shell. Internal or external shocks can heat the expanding gas up to temperatures of a few keV, leading to the emission of X-rays with a thermal plasma spectrum. Finally, when accretion is reestablished in the cataclysmic variable, the accretion flow is responsible for the emission of X-rays, also with a thermal plasma spectrum.

A systematic search for X-ray emission of classical novae was performed by Orio et al. (2001a) in the ROSAT archival data, which contained observations of 108 classical and re-current novae, 39 of which were less than 10 years old. Contrary to expectations, just a few

novae were detected in X-rays, and only three of them with a soft X-ray spectrum: GQ Mus (Nova Mus 1983, already discovered by EXOSAT in 1983, Ögelman (1984)), V1974 Cyg (Nova Cyg 1992, Krautter et al. (1996); Balman et al. (1998)), and Nova LMC 1995 (Orio & Greiner 1999). GQ Mus is renowned for having the longest soft X-ray emission phase (around 9 years; Ögelman et al. (1993); Shanley et al. (1995); Balman & Krautter (2001)). Other novae were detected in X-rays with ROSAT, but without any soft component: V351 Pup (Nova Pup 1991, Orio et al. (1996)), and V838 Her (Nova Her 1991, Lloyd et al. (1992); O’Brien et al. (1994)). Finally, only 11 out of the 81 galactic quiescent novae observed by ROSAT were detected in hard X-rays. For all these non soft X-ray sources, the poor spectral resolution and/or limited spectral range of the detectors left the origin of the emission (either shocked ejecta or reestablished accretion) unclear.

After the ROSAT era, observations by Beppo-SAX and Chandra revealed new interesting results. A soft component was reported for V382 Vel (Nova Vel 1999) which lasted for 7.5–8 months and contained a wealth of emission lines never previously detected in novae (Orio et al. 2002; Burwitz et al. 2002). In the case of V1494 Aql (Nova Aql 1999 No.2), a soft component appeared 6–10 months after the explosion, with a puzzling light curve including a short burst and oscillations (Drake et al. 2003). Observations of the recurrent nova CI Aql by Greiner & Di Stefano (2002) showed a soft component, but its spectrum implied an emitting radius of only 40 km for this source, which is too small for a white dwarf. In addition, supersoft X-ray emission 6 months after outburst, with strong temporal variation was reported by Ness et al. (2003) and Petz et al. (2005) for V4743 Sgr (Nova Sgr 2002 No.3).

XMM-Newton also contributed with some more observations of novae. X-ray emission with a soft spectrum was detected from Nova LMC 1995 by Orio et al. (2003) more than 5.5 years after the explosion. This component was not detected in later observations by Orio (2004) in 2003. X-rays were also detected from Nova LMC 2000 by Greiner et al. (2003) on days 17 and 51 after outburst, with a thermal plasma emission related to the ejecta and fading away on day 294. Finally, in the case of V2487 Oph (Nova Oph 1998), Hernanz & Sala (2002) detected X-ray emission with a broad thermal plasma spectrum extending up to ~ 10 keV and a fluorescent Fe K_α line, clearly indicating the reestablishment of accretion in a magnetic cataclysmic variable.

X-ray observations of classical novae during their post-outburst stages provide crucial information about the nova phenomenon (Orio 1999; Orio 2004; Krautter 2002): soft X-rays yield a unique insight into the remaining nuclear burning on top of the white dwarf, while hard X-rays reflect the shocks in the ejecta in the post-outburst novae, and the properties of the accretion flow in the “quiescent novae”. In view of the scarcity of objects observed and the diversity of behaviours detected, only the monitoring of as many novae as possible, with

large sensitivity and spectral resolution (as those offered by XMM-Newton and Chandra) can help to understand and solve these issues. The observations of Nova Sgr 1998 with XMM-Newton reported in this paper contribute to achieve this goal. In §2 we describe the observations, and in §3 the spectral analysis of the data is explained in detail. Discussion follows in §4 and a summary in §5.

2. Observations

The X-Ray Multi-Mirror Mission, XMM-Newton, is an X-ray astrophysics observatory (see Jansen et al. (2001) for a general description) including three X-ray telescopes, each with an European Photon Imaging Camera (EPIC) at its focal plane, and an optical/UV telescope, OM (Mason et al. 2001). The detectors of two of the EPIC cameras use MOS CCDs (Turner et al. 2001), whereas the third one uses pn CCDs (Strüder et al. 2001). In addition, two Reflection Grating Spectrometers (den Herder et al. 2001) for high resolution X-ray spectroscopy are mounted in the light path of the two EPIC MOS cameras.

We observed Nova Sgr 1998 at three epochs, with intervals of 6 months between observations: October 11, 2000, March 9, 2001 and September 7, 2001 (i.e., 934, 1083 and 1265 days after outburst; see Table 1). Exposure times ranged from 6 ks to 9 ks. While the source was clearly detected with the EPIC MOS1, MOS2 and pn cameras, the signal to noise ratio was too small to detect it with the RGS instruments.

Data were reduced using the XMM-Newton Science Analysis System (SAS 6.5.0). Standard procedures described in the SAS documentation (Loiseau 2005; Snowden et al. 2004) were applied. New calibration files affecting the soft spectrum of observations of the first XMM-Newton cycle were released in January 2006 (Kirsch 2006), and the pipeline products of some exposures of our observations were not available in the archive. Therefore, we reprocessed the original Observation Data Files (ODFs) for all exposures using the most recent calibrations. Only events with pattern smaller than 12 (MOS) and 4 (pn) and with pulse height (PI) in the range 0.2–12 keV (MOS) and 0.2–15 keV (pn) were selected for spectral analysis. Flaring background periods affecting some EPIC-pn exposures were filtered by creating good time interval (GTI) filter tables that were used for further event select procedures. Source photons were extracted from a circle of 35", and the background was extracted from a region of the same area, close to the source but free from source photons, and keeping the same distance to the readout node (RAWY) as the source region (Kirsch 2006). The statistics of our observations were not good enough to perform timing analysis, which would have been interesting to determine the presence of some periodicity, as observed in the optical by Lipkin et al. (2001).

3. Spectral analysis

The X-Ray Spectral Fitting Package (XSPEC 11.3, Arnaud & Dorman (2003)) was used for spectral analysis. For each observation, the spectra of the three EPIC cameras (pn, MOS1 and MOS2) were simultaneously fitted. An absorbing column density compatible with or smaller than the interstellar value was obtained for all spectral models. A column density smaller than the interstellar N_{H} is clearly unphysical, and the spectral fits never indicate a larger value. Therefore, we froze it in all our fits to $N_{\text{H}} = 1.6 \times 10^{21} \text{cm}^{-2}$, which is the average interstellar column density in the direction of Nova Sgr 1998 (Dickey & Lockman 1990). This value is also consistent with the N_{H} derived from the measured extinction (Lynch et al. 2001), through the empirical relationship between interstellar X-ray absorption and optical extinction (Gorenstein 1975).

3.1. Spectral models

A first look at the data (Fig. 1) clearly shows that the emission spans the whole energy range of the EPIC instruments, 0.2 – 10 keV, with a spectrum harder than that produced by residual H-burning on top of the white dwarf. This immediately indicates that the emission must be dominated by either the hot ejected shell, or by a reestablished accretion flow. We thus fit the EPIC spectra with a multi-temperature optically thin thermal plasma, simulated with a Raymond-Smith model (Raymond & Smith 1977) in XSPEC. The main processes included in this model are bremsstrahlung, recombination continua and line emission. More sophisticated models such as MEKAL (Mewe et al. 1995) are senseless for our data, since these models require a larger number of parameters whereas we have a low number of counts. We checked, however, that the results obtained with MEKAL and Raymond-Smith models are similar. A single temperature thermal plasma model is completely unable to fit the data, because the emission spans a broad energy range. At least two components at different temperatures are needed to obtain a reasonable fit, with the best fit being obtained for a three-temperature model.

Since the thermal plasma emission can arise either in the ejecta or in the accretion flow, two kinds of chemical composition are possible: solar abundances (for an accretion flow), or metal enriched (for the nova ejecta). In this latter case, the underlying white dwarf of the nova can have two different compositions: carbon-oxygen (CO) for masses $\leq 1.15 M_{\odot}$, or oxygen-neon (ONe) for masses up to the Chandrasekhar limit. Here we use realistic compositions of the ejecta from José & Hernanz (1998). We tested their 14 ejecta compositions, corresponding to CO and ONe nova models with masses ranging from 0.8 to 1.15 M_{\odot} and 1.0 to 1.35 M_{\odot} , respectively, and degrees of mixing between accreted mass and

underlying core from 25 to 75 %. In general, the best fit is obtained for low-mass CO novae (see below for details).

We also considered the possible contribution of residual H-burning on the post-outburst white dwarf (again CO or ONe). We used white dwarf atmosphere emission models, gently provided by Jim MacDonald (MacDonald & Vennes 1991), and built tables to be read as external models in XSPEC. Previous studies have shown the importance of including white dwarf atmosphere models instead of simple blackbodies for a correct spectral analysis of novae or supersoft X-ray sources (Balman et al. 1998; Balman & Krautter 2001; Orio & Greiner 1999).

3.2. Results

A three temperature (3T) optically thin thermal plasma model provides a good fit for the three EPIC cameras spectra of the first observation. The fit is only slightly poorer for the third observation, while the poor statistics lead to a much worse fit at the second epoch. However, no other model provides a better fit and the physical origin of the emission is very likely to be the same in all our observations. Therefore, we fit the spectra at the three epochs with the same 3T plasma model.

Figure 1 (upper panel) shows Nova Sgr 1998 spectra in October 2000, 934 days (2.6 years) after the explosion, with the best fit model and the residuals in units of χ . The 3T plasma model provides a good fit to the EPIC MOS1, MOS2 and pn data, both simultaneously and individually. The 3T model was used only after checking that a two temperature plasma model (which would be preferred because of its simplicity) results in a worse fit (see Table 2), leaving significant residuals, in particular around 1 keV. We also attempted to fit the spectra with a cooling flow model, which is a good representation of a multi-temperature plasma in accretion disks in old novae (Mukai et al. 2003). However, the spectrum is not well fitted with this model: with $T_{\text{low}}=0.08$ keV, $T_{\text{high}}=3$ keV and normalization constant $10^{-9}M_{\odot}/\text{yr}$, the reduced χ^2 is 2.9; therefore we should rule out the cooling flow model for Nova Sgr 1998.

Table 3 shows the best-fit parameters for the 3T plasma models both with solar and with CO nova abundances. In both cases, the three temperatures are around 0.1, 0.8 and > 5 keV (probably indicating a continuous distribution between the two extremes). The main difference between the results with different abundances lies in the emission measures (EM, defined as $\int n_e n_i dV \simeq \int n_e^2 dV$, with n_e and n_i the electronic and ionic densities, respectively). The EM for the coolest component in the solar case is extremely large (by itself and when compared with the EM of the intermediate and high temperature components). But this

problem disappears when a CO plasma is considered, because the emission measure for the coolest component decreases by a factor of 100. The difference is due to the strong emission lines at energies at 0.1-1 keV for the C, N and O enriched abundances. Confidence contours for the parameters of the three components are displayed in Figure 2.

The presence of a soft X-ray atmospheric component in the spectrum of Nova Sgr 1998 can not be ruled out, but only upper limits can be established (Fig. 3). They include a broad confidence region of the $T_{\text{eff}}\text{-}L_{\text{bol}}$ parameters, but taking into account the path of a post-outburst nova on the $T_{\text{eff}}\text{-}L_{\text{bol}}$ diagram, we can conclude that hydrogen burning had already turned off by the time of our first observation. The initial evolution of a post-outburst nova follows a constant bolometric luminosity path (close to Eddington limit, i.e., $\sim 10^{38}\text{erg/s}$ for a $1M_{\odot}$ white dwarf) with increasing effective temperature (Kato & Hachisu 1994; Sala & Hernanz 2005b). If Nova Sgr 1998 had been in this first phase with high luminosity at the time of our observation, 2.7 years after the outburst, it would have been at high temperature. But for a high luminosity, the upper limits for our first observation are compatible only with low temperatures, which would indicate an extended envelope. This is highly unlikely for a nova 2.6 years after the outburst. Therefore we conclude that hydrogen burning had already turned-off by the time of our first observation. The upper limits are however compatible with a cooling white dwarf: taking 10^8cm as a hard lower limit for the radius of the degenerate star, Fig. 3 indicates that it was colder than $3 \times 10^5\text{K}$.

The second observation (3.0 years after the explosion, middle panel in Fig 1) provided lower signal to noise data (due to a smaller exposure time, $\sim 30\%$ less than in the first observation, Table 1). For completeness, we include a fit similar to that used for the first and third observations. Despite the large error ranges, the best-fit parameters (Table 3) indicate a slight softening of the spectrum, with lower temperatures for the first and third component.

The fit results for the third observation (3.5 years after the explosion, lower panel in Fig 1), are similar to the first one. However, the emission measures for the intermediate and highest temperature components are a bit smaller, whereas that associated with the coolest component is larger than one year before. This evolution is compatible with some cooling of the plasma between the first and third epochs.

4. Discussion

The optically thin thermal plasma emission may originate either in the shocked expanding nova shell or in the accretion flow. The problem of distinguishing between these two possi-

bilities has already been faced in the case of other sources: Nova Pup 1991 (Orio et al. 1996), Nova Her 1991 (Lloyd et al. 1992; O’Brien et al. 1994), Nova Cyg 1992 (Krautter et al. 1996; Balman et al. 1998), Nova Vel 1999 (Orio et al. 2001b; Mukai & Ishida 2001). We discuss below some properties of the models which could help to disentangle the origin of the emission: luminosity and emission measure (i.e., value and temporal evolution of electronic density).

The unabsorbed X-ray (0.2–10 keV) luminosity for Nova Sgr 1998 is in the range $10^{33} - 10^{34}$ erg/s in all cases, for a distance of 9 kpc (Lipkin et al. 2001). Distances to novae are quite uncertain, and Nova Sgr 1998 is not an exception ($d=8.9\pm2.5$ kpc), but a factor of ≤ 2 in distance only changes the luminosity by a factor of ≤ 4 . This luminosity is too large to originate from the accretion onto a non-magnetic white dwarf (typically $10^{29} - 10^{32}$ erg/s, Kuulkers et al. (2003)), or in a polar cataclysmic variable (with luminosities $\sim 10^{32}$ erg/s, Mukai (2003); Ramsay & Cropper (2004)). However, it could be related to accretion in an intermediate polar, with luminosities $\sim 10^{33}$ erg/s (Mukai 2003). In fact, optical observations suggested that Nova Sgr 1998 is a nearly synchronous magnetic system (Lipkin et al. 2001), and photometric observations of other post-novae indicate that some are intermediate polars (for instance, V697 Sco, Warner & Woudt (2002)).

The X-ray luminosity of Nova Sgr 1998 is also compatible with the observed values for nova ejecta. For example, Nova Her 1991 emitted $5 \times 10^{33} - 10^{35}$ erg/s only five days after outburst, fading afterwards extremely quickly (Lloyd et al. 1992; O’Brien et al. 1994); Nova Cyg 1992 ejecta X-ray emission reached $(0.8 - 2.0) \times 10^{34}$ erg/s around 150 days after outburst (Balman et al. 1998); Nova Pup 1991 emitted around 7.5×10^{33} erg/s 16 months after outburst (Orio et al. 1996); and Nova Vel 1999 also reached $L > 10^{34}$ erg/s in the band above 0.8 keV 15 days after maximum (the shell luminosity was even larger, since emission lines detected below 0.8 keV also originated in the ejecta), but it decreased to a few 10^{33} erg/s 5.5 months later (Orio et al. 2001b, 2002). In all those previous cases the ejecta cooled much faster than in Nova Sgr 1998. However, the expected cooling time for the electronic densities, n_e , in nova ejecta (in general smaller than 10^6cm^{-3}) are larger than 10 years (Brecher et al. 1977; Ögelman 1987). Therefore, X-ray emission from shock heated ejecta in Nova Sgr 1998 3.5 years after the outburst would be fully compatible with theoretical predictions of cooling times.

For a shock-heated plasma, temperatures are related to velocity as $kT \propto v^2$ (Brecher et al. 1977). For the expansion velocities observed by Lynch et al. (2001) (1800 km/s, on days 525 and 850 after outburst), the plasma temperature would be ~ 3 keV, which lies within the range of temperatures of our best-fit thermal plasma models. Coronal lines, which are a good signature of shocks in the plasma, were also present in those observations, supporting the presence of a shocked ejecta in Nova Sgr 1998. Assuming an expansion at constant velocity,

the emission volume at the time of our observations would be increasing from $1.3 \times 10^{49} \text{ cm}^3$ (for day 934) to $3.2 \times 10^{49} \text{ cm}^3$ (day 1265). With these volumes and the emission measures for CO models from Table 3, electronic densities, n_e , in the shell would evolve from $1.5 \times 10^3 \text{ cm}^{-3}$ (day 934) to $1.3 \times 10^3 \text{ cm}^{-3}$ (day 1265) for the coolest component. Similarly, n_e decreases from 10^3 cm^{-3} to 500 cm^{-3} , and from $2 \times 10^3 \text{ cm}^{-3}$ to 10^3 cm^{-3} for the intermediate and high temperature components, respectively. Since the spherical geometry gives the maximum emitting volume, these n_e are lower limits. The small n_e agree with the thinning of the ejecta found between days 525 and 850 by Lynch et al. (2001).

The electronic density in a spherical shell with its outer radius expanding at constant velocity evolves with time as t^{-3} , while in an expanding shell of constant thickness n_e evolves as t^{-2} (Lyke et al. 2003). With the first expansion picture, a decrease of n_e by a factor $\sim 2.5 = 1/0.4$ is expected between the first and the third observations, while the decay would be by a factor of $\sim 1.8 = 1/0.5$ in the second case. For Nova Sgr 1998, the n_e derived above for the CO model changes by a factor of 0.8 for the coolest thermal plasma component. For the intermediate and hottest components n_e decreases by 0.5, the expected factor for an expanding shell of constant thickness. Therefore, the n_e evolution also supports the expanding ejecta as the possible site of the observed X-ray emission. However, the large errors associated with n_e (in particular for the lowest temperature component) prevent a clear conclusion about the shell geometry.

5. Summary

The X-ray spectrum of Nova Sgr 1998 as observed by XMM-Newton between 2.6 and 3.5 years after outburst is dominated by thermal plasma emission. The best-fit is obtained with a three-component thermal plasma model, with temperatures between 0.1 and 40 keV. Thermal plasma models with different compositions (solar, and several abundances from realistic nova ejecta) have been tried. The best-fit is obtained with either the abundances of a CO nova shell (for $0.8 M_\odot$ and 25% mixing), or with solar abundances. The first case would correspond to emission from the expanding nova shell, while the second would be associated with reestablished accretion in the cataclysmic variable.

The X-ray luminosity, the values of the plasma temperatures, the chemical composition, and the distribution and evolution of emission measures point to shock heated ejecta as the most likely origin for the plasma emission, rather than resumed accretion in the cataclysmic variable. Also the inability to fit the data with a cooling flow model casts doubts on accretion as the origin of the X-ray emission. Finally, the spectra of Nova Sgr 1998 do not show any fluorescence iron line, contrary to what was observed for V2478 Oph (Hernanz & Sala 2002),

which clearly indicated that accretion was reestablished in the cataclysmic variable.

Regarding the presence of residual hydrogen burning on the white dwarf surface, our observations indicate that the post-outburst nova envelope had already turned off its hydrogen burning already 2.6 years after optical maximum.

We thank Jim MacDonald for kindly providing his white dwarf atmosphere models, and the referee for many helpful comments, which have considerably improved this paper. This work is based on observations obtained with XMM-Newton, an ESA science mission with instruments and contributions directly funded by ESA Member States and NASA. The XMM-Newton project is supported by the Bundesministerium für Wirtschaft und Technologie/Deutsches Zentrum für Luft- und Raumfahrt (BMWi/DLR, FKZ 50 OX 0001), the Max-Planck Society and the Heidenhain-Stiftung. This research has made use of the SIMBAD database, operated at CDS, Strasbourg, France, and has been partially funded by the Spanish Ministry for Education and Science (MEC) project AYA2004-06290-C02-01 and by FEDER. G.S. is supported through a postdoctoral fellowship from the MEC.

REFERENCES

- Arnaud, K., Dorman, B. 2003, XSPEC User's Guide for Version 11.3.x, (HEASARC, NASA/GSFC, Greenbelt, MD)
- Balman, S., Orio, M. & Ögelman, H. 1995, ApJ, 449, L47
- Balman, S., Krautter, J. & Ögelman, H. 1998, ApJ, 499, 395
- Balman, S. & Krautter, J. 2001, MNRAS, 326, 1441
- Balman, S. & Ögelman, H. 1999, ApJ, 518, L111
- Brecher, K., Ingham, W.H., Morrison, P. 1977, ApJ, 213, 492
- Burwitz, V, Starrfield, S., Krautter, J., Ness, J.U. 2002 in Classical Nova Explosions, eds. M. Hernanz & J. José, AIP Conference Proceedings 637, p.386
- Della Valle M., Pizzella A., Bernardi M., Jones A.F., Kiss L., Hornoch K., Schmeer P., Trigo J.M. 1998, IAUC 6848
- den Herder, J.W. et al. 2001, A&A, 365, L7
- Dickey, J.M., Lockman, F.J. 1990, ARAR, 28, 215

- Drake, J., Wagner, R. M., Starrfield, S., Butt, Y., Krautter, J., Bond, H. E., Della Valle, M., Gehrz, R. D., Woodward, C. E., Evans, A., Orio, M., Hauschildt, P., Hernanz, M., Mukai, K., Truran, J. W. 2003, *ApJ*, 584, 448
- Gehrz, R.D., Truran, J.W., Williams, R.E., Starrfield, S. 1998, *PASP*, 110, 3
- Gorenstein, P. 1975, *ApJ*, 198, 95
- Greiner, J. & Di Stefano, R. 2002, *ApJ*, 578, L59
- Greiner, J., Orio, M. & Schartel, N. 2003, *A&A*, 405, 703
- Hernanz, M. & Sala, G. 2002, *Science*, 298, 393.
- Ikeda, Y., Kawabata, K.S., Akitaya, H. 2000, *A&A*, 355, 256
- Jansen, F. et al. 2001, *A&A*, 365, L1
- José, J., Hernanz, M. 1998, *ApJ*, 494, 680
- Kato, M., Hachisu, I. 1994, *ApJ*, 437, 802
- Kirsch, M. 2006, EPIC status of calibration and data analysis, XMM-SOC-CAL-TN-0018 (ESA-ESAC, XMM-Newton SOC)
- Krautter, J. 2002, in *Classical Nova Explosions*, eds. M. Hernanz & J. José, AIP Conference Proceedings 637, p.345
- Krautter, J., Ögelman, H., Starrfield, S., Wichmann, R. & Pfeffermann, E. 1996, *ApJ*, 456, 788
- Kuulkers, E., Norton, A., Schwope, A., Warner, B. 2003, in *Compact stellar X-ray sources*, eds. W.H.G. Lewin, M. van der Klis, Cambridge University Press (in press; astro-ph/0302351)
- Liller, W. 1998, *IAUC* 6846
- Liller, W., Jones, A.F. 1999, *IBVS*, 4664, 1
- Lipkin, Y., Leibowitz, E.M., Retter, A., Shemmer, O. 2001, *MNRAS*, 328, 1169
- Lloyd, H. M., O’Brien, T. J., Bode, M. F., Predehl, P., Schmitt, J.H.M.M., Trmper, J., Watson, M.G. & Pounds, K. A. 1992, *Nature*, 356, 222

- Loiseau, N. 2005, Users' Guide to the XMM-Newton Science Analysis System, Issue 3.2, (ESA/XMM-Newton Science Operations Centre, VILSPA, Madrid)
- Lyke, J.E., Koenig, X. P., Barlow, M. J., Gehrz, R. D., Woodward, C. E., Starrfield, S., Péquignot, D., Evans, A., Salama, A., González-Riestra, R., Greenhouse, M.A., Hjellming, R. M., Jones, T.J., Krautter, J., Ögelman, H. B., Wagner, R. M., Lumsden, S. L., Williams, R. E. 2003, AJ, 126, 993
- Lynch, D.K., Rudy, R.J., Venturini, C.C., Makuz, S. 2001, AJ, 122, 2013
- Mac Donald, J. & Vennes, S., 1991, ApJ, 373, L51
- Mason, K.O. et al. 2001, A&A, 365, L36
- Mewe, R., Kaastra, J.S., Liedhal, D.A., 1995, Legacy 6, 16 (available at <http://heasarc.gsfc.nasa.gov/docs/journal/meke6.html>)
- Mukai, K., Ishida, M. 2001, ApJ, 551, 1024
- Mukai, K. 2003, AdSpR, 32, 2067
- Mukai, K., Kinkhabwala, A., Peterson, J.R., Kahn, S.M. & Paerels, F. 2003, ApJ, 586, 77
- Ness, J.-U., Starrfield, S., Burwitz, V., Wichmann, R., Hauschildt, P., Drake, J.J., Wagner, R.M., Bond, H.E., Krautter, J., Orío, M., Hernanz, M., Gehrz, R. D., Woodward, C. E., Butt, Y., Mukai, K., Balman, S., Truran, J. W. 2003, ApJ, 594, L127
- O'Brien, T.J.O., Lloyd, H.M., Bode, M.F. 1994, MNRAS, 271, 155
- Ögelman, H., Beuermann, K. & Krautter, J. 1984, ApJ, 287, L31
- Ögelman, H., Krautter, J. & Beuermann, K. 1987, A&A, 177, 110
- Ögelman, H., Orío, M., Krautter, J. & Starrfield, S. 1993, Nature, 361, 331
- Orío, M. 1999, Physics Reports, 311, 419
- Orío, M., Balman, S., Della Valle, M., Gallagher, J. & Ögelman, H. 1996, ApJ, 466, 410
- Orío, M. & Greiner, J. 1999, A&A, 344, L13
- Orío, M., Covington, J. & Ögelman, H. 2001a, A&A, 373, 542
- Orío, M., Parmar, A.N., Benjamin, R., Amati, L., Frontera, F., Greiner, J., Ögelman, H., Mineo, T., Starrfield, S., Trussoni, E. 2001b, MNRAS, 326, L13

- Orio, M., Parmar, A.N., Greiner, J., Ögelman, H., Starrfield, S., Trussoni, E. 2002, MNRAS, 333, L11
- Orio, M., Hartmann, E., Still, M., Greiner, J. 2003, ApJ, 594, 435
- Orio, M., 2004, RMXAA, 20, 182
- Petz, A., Hauschildt, P.H., Ness, J.-U., Starrfield, S. 2005, A & A, 431, 321
- Ramsay, G. & Cropper, M. 2004, MNRAS, 347, 497
- Raymond, J. & Smith, B. 1977, ApJ Suppl, 35, 419
- Sala, G. & Hernanz, M. 2005a, A&A, 439, 1057.
- Sala, G. & Hernanz, M. 2005b, A&A, 439, 1061
- Shanley, L., Ögelman, H., Gallagher, J. S., Orio, M. & Krautter, J. 1995, ApJ, 438, L95
- Snowden, S., Immler, S., Arida, M., Perry, B., Still, M., Harrus, I., 2004, An Introduction to XMM-NEWTON Data Analysis, Version 2.01 (NASA/GSFC XMM-Newton Guest Observer Facility, Greenbelt, MD)
- Starrfield, S. 1989, in Classical Novae, Wiley, New York, p. 39
- Strüder, L.. et al. 2001, A&A, 365, L18
- Tuchman, Y. & Truran, J.W. 1998, ApJ, 503, 381
- Turner, M.J.L. et al. 2001, A&A, 365, L27
- Warner, B., Woudt, P. 2002, PASP, 114, 1222
- Williams, R. 1992, AJ, 104, 725

Table 1. Observation log.

Observation Date (orbit)	Time after Discovery	EPIC pn		EPIC MOS1		EPIC MOS2	
		Exposure Time (s)	Count Rate (10^{-2} cts s^{-1})	Exposure Time (s)	Count Rate (10^{-2} cts s^{-1})	Exposure Time (s)	Count Rate (10^{-2} cts s^{-1})
Oct.11, 2000 (154)	934 d, 2.6 yr	6213	10.1 ± 0.5	9048	2.4 ± 0.2	9051	2.7 ± 0.2
Mar. 9, 2001 (229)	1083 d, 3.0 yr	3058	8.6 ± 0.6	6575	2.1 ± 0.2	6575	2.2 ± 0.2
Sep. 7, 2001 (320)	1265 d, 3.5 yr	5883	8.2 ± 0.4	9086	2.0 ± 0.2	9086	1.9 ± 0.2

Table 2. Parameters of the fit for each one of the three observations of Nova Sgr 1998, with a two temperatures thermal plasma (Raymond-Smith), with solar and CO1 abundances.

	1 st Observation	2 nd Observation	3 rd Observation
Solar abundances			
kT_{RS1} (keV)	$0.12 - 0.20$	$0.03 - 0.06$	$0.06 - 0.12$
$EM_{RS1}(\times 10^{57} \text{cm}^{-3})$	$0.07 - 0.27$	$20 - 2000$	$0.3 - 11.3$
kT_{RS2} (keV)	$4 - 11$	$2 - 16$	$2 - 6$
$EM_{RS2}(\times 10^{55} \text{cm}^{-3})$	$12 - 15$	$6 - 10$	$8 - 12$
$F_{\text{unabs}, 0.2-10.0 \text{ keV}}(\times 10^{-13} \text{erg cm}^{-2} \text{s}^{-1})$	$4 - 7$	$2 - 210$	$2 - 30$
$L_{\text{unabs}, 0.2-10.0 \text{ keV}}(\times 10^{33} \text{erg s}^{-1})$	$4 - 7$	$2 - 203$	$2 - 29$
χ^2_{ν}	1.55	2.07	1.66
CO abundances			
kT_{RS1} (keV)	$0.09 - 0.19$	$0.03 - 0.07$	$0.07 - 0.15$
$EM_{RS1}(\times 10^{55} \text{cm}^{-3})$	$0.3 - 1.7$	$10 - 3 \times 10^4$	$0.4 - 4.4$
kT_{RS2} (keV)	$3 - 8$	$1 - 6$	$2 - 6$
$EM_{RS2}(\times 10^{55} \text{cm}^{-3})$	$5 - 6$	$1 - 4$	$2 - 5$
$F_{\text{unabs}, 0.2-10.0 \text{ keV}}(\times 10^{-13} \text{erg cm}^{-2} \text{s}^{-1})$	$4 - 6$	$1 - 80$	$2 - 6$
$L_{\text{unabs}, 0.2-10.0 \text{ keV}}(\times 10^{33} \text{erg s}^{-1})$	$4 - 6$	$1 - 77$	$2 - 6$
χ^2_{ν}	1.37	2.01	1.57

Note. — The best-fit models shown fit simultaneously the data from the three EPIC cameras. All the limits are 3σ . The emission measures and luminosities are given for a distance $d=9\text{kpc}$; a factor $(d/9\text{kpc})^2$, with d the distance in kpc, affects these magnitudes. The absorption N_{H} is $1.6 \times 10^{21} \text{cm}^{-2}$ everywhere.

Table 3. Parameters of the best-fit model for each one of the three observations of Nova Sgr 1998: three temperatures thermal plasma (Raymond-Smith), with solar and CO1 abundances.

	1 st Observation	2 nd Observation	3 rd Observation
Solar abundances			
$kT_{\text{RS1}}(\text{keV})$	$0.07 - 0.16$	$0.03 - 0.05$	$0.06 - 0.10$
$EM_{\text{RS1}}(\times 10^{57} \text{cm}^{-3})$	$0.1 - 2.4$	$50 - 5000$	$0.5 - 6.4$
$kT_{\text{RS2}}(\text{keV})$	$0.6 - 1.0$	$0.2 - 0.7$	$0.2 - 1.0$
$EM_{\text{RS2}}(\times 10^{55} \text{cm}^{-3})$	$0.9 - 3.7$	$0.5 - 3.9$	$0.4 - 2.0$
$kT_{\text{RS3}}(\text{keV})$	≥ 5	≥ 2	≥ 3
$EM_{\text{RS3}}(\times 10^{55} \text{cm}^{-3})$	$8 - 14$	$5 - 10$	$6 - 10$
$F_{\text{unabs}, 0.2-10.0 \text{ keV}}(\times 10^{-13} \text{erg cm}^{-2} \text{s}^{-1})$	$3 - 13$	$2 - 640$	$2 - 33$
$L_{\text{unabs}, 0.2-10.0 \text{ keV}}(\times 10^{33} \text{erg s}^{-1})$	$3 - 13$	$2 - 620$	$2 - 32$
χ^2_{ν}	1.16	1.40	1.22
CO abundances			
$kT_{\text{RS1}}(\text{keV})$	$0.07 - 0.15$	$0.02 - 0.07$	$0.05 - 0.13$
$EM_{\text{RS1}}(\times 10^{55} \text{cm}^{-3})$	$0.3 - 5.8$	$14 - 500000$	$0.5 - 11.0$
$kT_{\text{RS2}}(\text{keV})$	$0.6 - 1.1$	$0.4 - 1.2$	$0.4 - 1.1$
$EM_{\text{RS2}}(\times 10^{55} \text{cm}^{-3})$	$0.6 - 2.0$	$0.4 - 1.9$	$0.2 - 1.7$
$kT_{\text{RS3}}(\text{keV})$	≥ 5	≥ 2	≥ 3
$EM_{\text{RS3}}(\times 10^{55} \text{cm}^{-3})$	$3 - 7$	$1 - 5$	$2 - 5$
$F_{\text{unabs}, 0.2-10.0 \text{ keV}}(\times 10^{-13} \text{erg cm}^{-2} \text{s}^{-1})$	$2 - 8$	$1 - 5500$	$2 - 6$
$L_{\text{unabs}, 0.2-10.0 \text{ keV}}(\times 10^{33} \text{erg s}^{-1})$	$2 - 8$	$1 - 5300$	$2 - 6$
χ^2_{ν}	0.92	1.61	1.25

Note. — Same comments as in table 2.

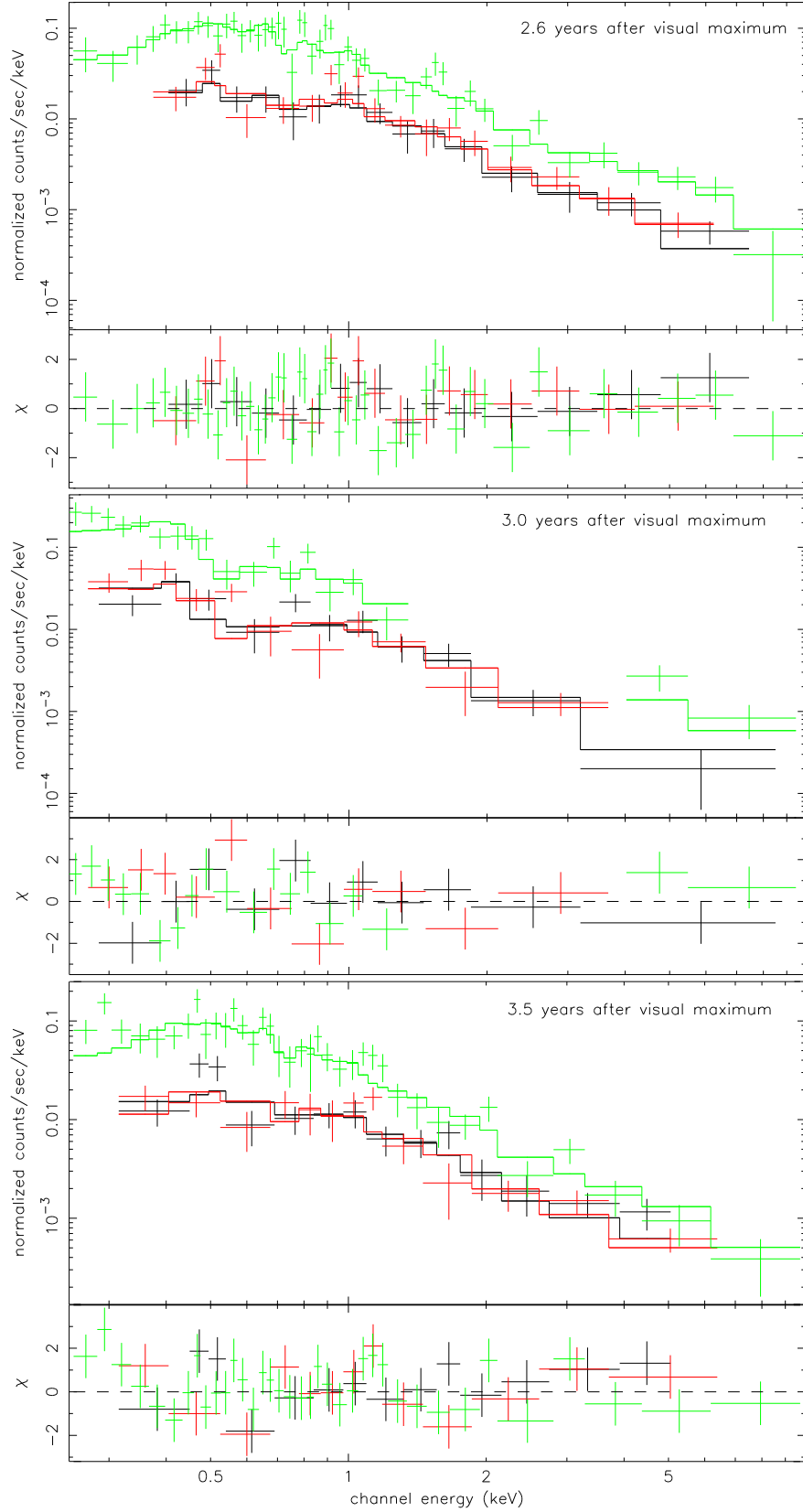


Fig. 1.— Nova Sgr 1998 EPIC MOS1 (black), MOS2 (red) and pn (green) observed spectra, with the best fit model (with CO abundances) and the residuals. From top to low panels: first, second and third observations.

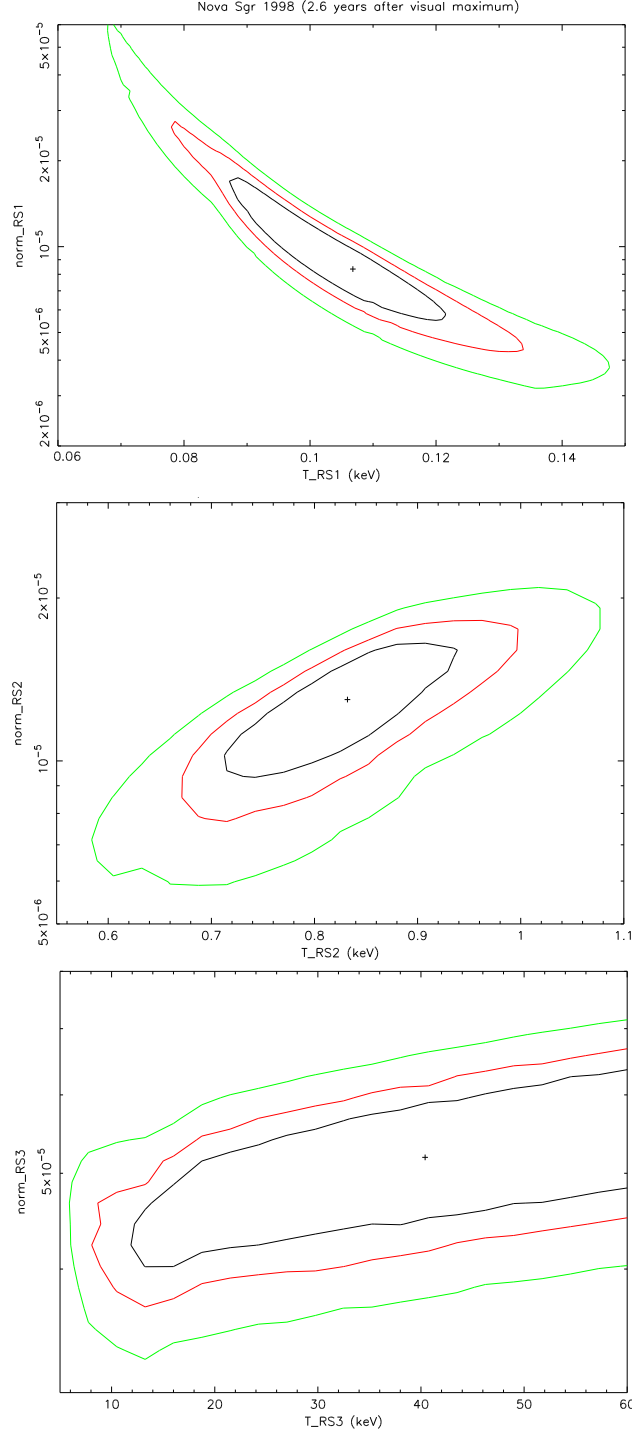


Fig. 2.— Confidence contours (1-innermost-, 2, and 3 -outermost- σ) for the temperature and normalization constant ($\text{norm}_{\text{RS}} = 10^{-14} \text{EM}/(4\pi D^2)$, where EM is the emission measure and D the distance in cm) of the low (upper panel), intermediate (middle panel) and high (lower panel) temperature thermal plasma components, for the models with CO abundances corresponding to the first observation of Nova Sgr 1998.

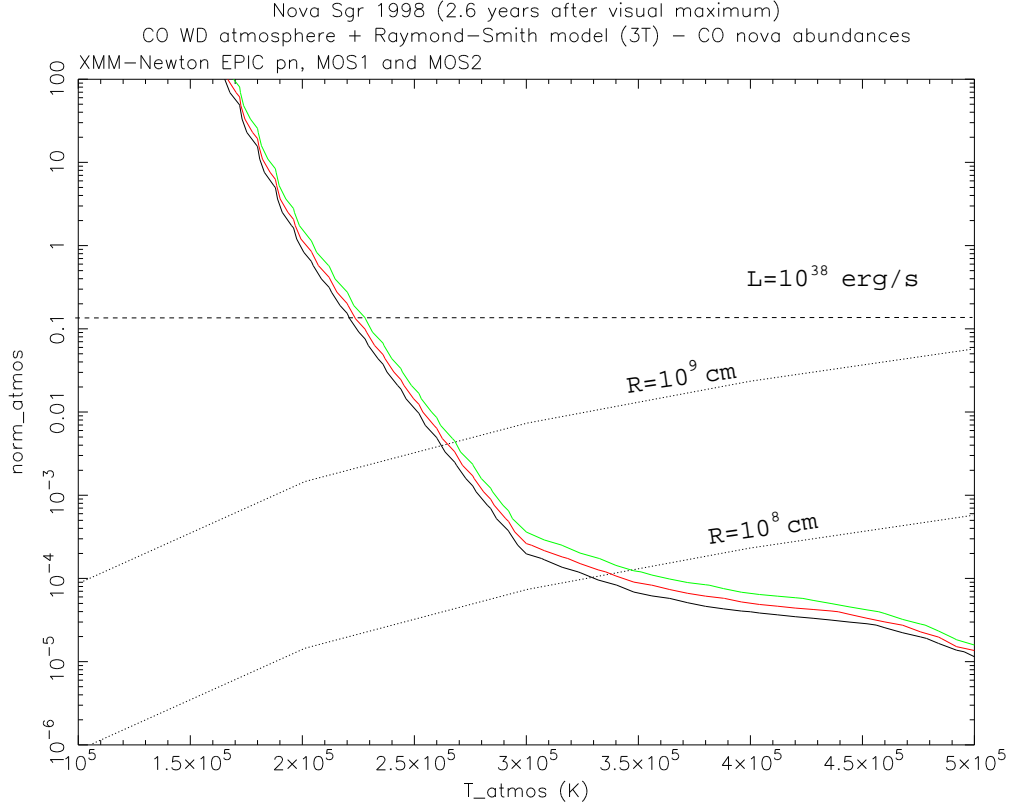


Fig. 3.— Upper limits (from left to right, 1, 2, and 3 σ confidence) for the effective temperature (T_{atmos}) and normalization ($\text{norm}=L_{39}/D_{10}^2$, where L_{39} is the luminosity in units of 10^{39}erg/s and D_{10} the distance to the source in units of 10 kpc) of the CO white dwarf atmosphere component (first observation). The thermal plasma model has three components and abundances corresponding to CO novae ejecta, as in previous figures. The luminosity of the nova during the constant bolometric luminosity phase, $L \sim 10^{38} \text{ erg/s}$ (dashed line), as well as the locii of constant white dwarf radius equal to 10^8 and 10^9 cm (dotted lines) are also displayed.